DOI: 10.1002/cbic.201300187

DXP Synthase-Catalyzed C–N Bond Formation: Nitroso Substrate Specificity Studies Guide Selective Inhibitor Design

Francine Morris,[a] Ryan Vierling,[a] Lauren Boucher,[b] Jürgen Bosch,[b] and Caren L. Freel Meyers*[a]

1-Deoxy-D-xylulose 5-phosphate (DXP) synthase catalyzes the first step in the nonmammalian isoprenoid biosynthetic pathway to form DXP from pyruvate and D-glyceraldehyde 3-phosphate (D-GAP) in a thiamin diphosphate-dependent manner. Its unique structure and mechanism distinguish DXP synthase from its homologues and suggest that it should be pursued as an anti-infective drug target. However, few reports describe any development of selective inhibitors of this enzyme. Here, we reveal that DXP synthase catalyzes C–N bond formation and exploit aromatic nitroso substrates as active site probes. Substrate specificity studies reveal a high affinity of DXP synthase for aromatic nitroso substrates compared to the related ThDP-dependent enzyme pyruvate dehydrogenase (PDH). Results from inhibition and mutagenesis studies indicate that nitroso substrates bind to *E. coli* DXP synthase in a manner distinct from that of D-GAP. Our results suggest that the incorporation of aryl acceptor substrate mimics into unnatural bisubstrate analogues will impart selectivity to DXP synthase inhibitors. As a proof of concept, we show selective inhibition of DXP synthase by benzylacetylphosphonate (BnAP).

Introduction

The isoprenoids are a vast and structurally diverse class of natural products derived from two simple bioprecursors, isopentenyl diphosphate (IDP) and dimethylallyl diphosphate (DMADP). Essential in all living organisms, isoprenoids are biosynthesized through two distinct pathways. The mevalonate pathway for IDP and DMADP biosynthesis is found in mammals and fungi. In contrast, most human pathogens, including many bacterial pathogens[1] and the malaria parasite, *Plasmodium falciparum*,[2] are known to use the methylerythritol phosphate (MEP) pathway (Scheme 1) for the generation of IDP and DMADP.[3] Its essentiality and prevalence in human pathogens, and absence in mammals, renders the MEP pathway a target for the development of new anti-infective agents, which are desperately needed to combat the emergence and re-emergence of drug resistance.

Seven biosynthetic steps make up the MEP pathway, beginning with the formation of 1-deoxy-D-xylulose 5-phosphate (DXP) from pyruvate (donor substrate) and D-glyceraldehyde 3-phosphate (D-GAP, acceptor substrate). This first transformation is catalyzed by DXP synthase in a thiamin diphosphate (ThDP)-dependent manner,[4] and is believed to play a regulatory role in isoprenoid biosynthesis.[5–8] In addition, DXP synthase is a branch point in pathogen metabolism.[4,9,10] Its product, DXP, is required for IDP/DMADP biosynthesis and is also a precursor in pyridoxal biosynthesis and, notably, ThDP biosynthesis, which is required for the formation of DXP itself.

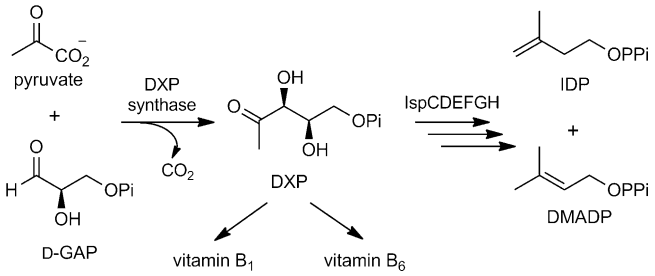

Scheme 1. Biosynthesis of isoprenoids IDP and DMADP through the methylerythritol phosphate (MEP) pathway.

The importance of DXP synthase in pathogen metabolism highlights this enzyme as a particularly interesting new drug target. Additionally, DXP synthase is mechanistically distinct from other ThDP-dependent enzymes. The enzyme combines decarboxylase and carboligase chemistry in a ThDP-dependent condensation of pyruvate and D-GAP (Scheme 1). A report by Eubanks et al.[11] provided compelling evidence for a unique catalytic mechanism in which binding of both acceptor and donor substrates is required to induce decarboxylation of pyruvate to form a kinetically competent ternary complex. In subsequent studies,[12,13] we have provided further support for the formation of a ternary complex during DXP synthase catalysis and D-GAP-promoted decarboxylation of the C2 α-lactylthia-

[a] F. Morris, R. Vierling, Prof. C. L. Freel Meyers
Department of Pharmacology and Molecular Sciences
The Johns Hopkins University School of Medicine
725 North Wolfe St, Baltimore, MD 21205 (USA)
E-mail: cmeyers@jhmi.edu

[b] L. Boucher, Prof. J. Bosch
Department of Biochemistry and Molecular Biology
The Johns Hopkins Malaria Research Institute
Bloomberg School of Public Health
615 North Wolfe Street, Baltimore, MD 21205 (USA)

Supporting information for this article is available on the WWW under http://dx.doi.org/10.1002/cbic.201300187.

min diphosphate (LThDP) intermediate, the pre-decarboxylation intermediate formed by reaction of pyruvate and ThDP. In contrast, all other ThDP-dependent enzymes are believed to follow classical ping-pong kinetics in which the activation of pyruvate and the release of carbon dioxide precede binding of the acceptor substrate.[14,15] In addition, structural analysis indicates that DXP synthase has a unique domain arrangement in which the active site is between domains of the same monomer within the homodimer.[16] This is in contrast to its homologues, in which the active site is at the dimer interface.[14,16] Taken together, these observations highlight unique aspects of DXP synthase catalysis and structure that distinguish it from its mammalian homologues, and suggest that it should be possible to selectively target this enzyme so as to develop new anti-infective agents. However, reports describing the development of selective DXP synthase inhibitors are scarce,[17,18] likely due to a perception that selective inhibition of DXP synthase over mammalian ThDP-dependent enzymes will be difficult,

We have pursued substrate specificity studies of DXP synthase to try to reveal important substrate binding determinants that could guide selective inhibitor design. Previously, we have shown that aliphatic aldehydes are accepted as alternative substrates to give the corresponding α-hydroxy ketones;[19] this suggests that DXP synthase displays some flexibility toward nonphosphorylated acceptor substrates. A subsequent study revealed the selective inhibitory activity of a series of alkylacetylphosphonates designed to act as unnatural bisubstrate analogues targeting a conformation of DXP synthase that uniquely accommodates both a donor and acceptor substrate in the formation of a ternary complex.[18] The largest alkylacetylphosphonate, butylacetylphosphonate, exhibited greater selectivity of inhibition than ethyl- and methylacetylphosphonates, thus indicating that selective targeting of DXP synthase is possible.

In this study, we explore the capacity of DXP synthase to bind sterically demanding scaffolds by evaluating its usage of aromatic acceptor substrates. We demonstrate the capacity of DXP synthase to catalyze the formation of C–N bonds to generate aromatic hydroxamic acids or amides from nitroso substrates. The intrinsically higher reactivity of nitroso substrate analogues compared to their aldehyde counterparts has permitted a substrate specificity study revealing aromatic substrates with high affinity for the enzyme. Further, our results suggest aromatic substrates might adopt a different binding mode from D-GAP in a relatively large active site compared to that of pyruvate dehydrogenase (PDH) or transketolase (TK). These results have prompted the design and synthesis of a DXP synthase inhibitor bearing an aromatic component to impart selectivity.

Results

Aromatic aldehydes as DXP synthase substrates

Some ThDP-dependent enzymes are known to catalyze C–C bond formation by using aromatic substrates with various turnover efficiencies;[20–22] however, there are no reports describing the use of aromatic substrates by DXP synthase. We tested several aromatic aldehydes as acceptor substrates, of which 2-hydroxy-4,6-dinitrobenzaldehyde appeared to be amongst the best, this was therefore fully characterized as a substrate for DXP synthase (Figure S1). It has a K_m of (512 ± 20) μM, approximately 18 times higher than that of the natural substrate, D-GAP, and its k_{cat} is low (k_{cat} = (0.35 ± 0.05) min^{-1}). The aromatic aldehyde study suggested that there might be flexibility in the active site of DXP synthase toward aromatic acceptor substrates (data not shown). However, a significant number of aromatic aldehydes are not turned over by DXP synthase; this suggests that the low intrinsic reactivity of aromatic aldehydes is a limiting factor in substrate specificity studies to probe the enzyme active site.

DXP synthase-catalyzed C–N bond formation

The nitroso group is a functional isostere of the aldehyde group and is known to possess higher reactivity toward nucleophiles. In fact, the ThDP-utilizing enzymes TK, pyruvate decarboxylase (PDC), benzaldehyde lyase (BAL) and PDH have been shown to use aromatic nitroso analogues as acceptor substrates in the formation of hydroxamic acids.[23–26,27a,b] We hypothesized that a substrate specificity study of DXP synthase with the intrinsically more reactive aromatic nitroso compound class would better inform us about key binding elements of aromatic substrates. In addition, we postulated that such a study could reveal a new application of DXP synthase as a biocatalyst for the generation of the medicinally important hydroxamic acid class.

Thus, a series of aromatic nitroso analogues was tested as substrates for DXP synthase. Notably, DXP synthase turns over a range of structurally diverse nitroso substrates (**1**, **3**–**9**, Scheme 2); most aldehyde counterparts of these nitroso analogues are not substrates for the enzyme; this is consistent

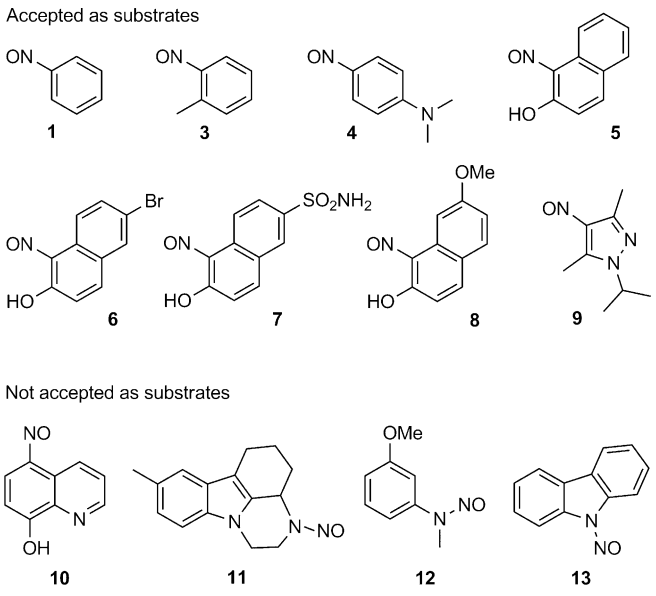

Scheme 2. Nitroso substrate usage by DXP synthase.

with the idea that the nitroso isostere is more reactive. A representative HPLC stack plot that illustrates DXP synthase-catalyzed conversion of the simplest aromatic nitroso analogue, nitrosobenzene (**1**), to the corresponding hydroxamic acid (**2**) is shown in Figure 1 (see also Figure S2). A single C-nitroso ana-

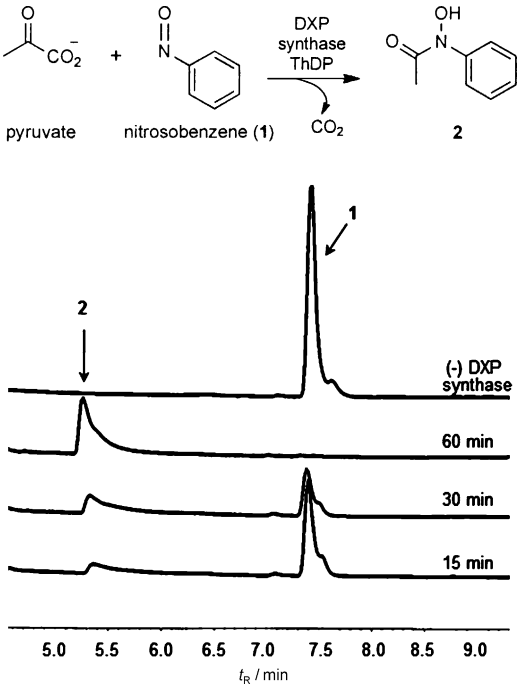

Figure 1. HPLC analysis of the DXP-synthase-dependent conversion of nitrosobenzene to hydroxamic acid **2**.

logue, **10**, did not act as substrate for the enzyme; neither were N-nitroso compounds substrates. The electron-rich *p*-dimethylamino nitroso analogue **4** is a substrate for DXP synthase (Figure S4), but not for yeast TK.[26] Interestingly, the corresponding amides, presumably produced through a mechanism involving the unstable hydroxamic acid as an intermediate,[25] were detected as the major products of several electron-rich substrates (**4**–**8**, Scheme 2, Figures S4–S8)). This result has been reported in a study that examined the turnover of **4** by PDC.[25] However, the observation that the amide is also isolated from naphthol substrates was unexpected. In order to rule out the possibility that bovine serum albumin (BSA) added to enzymatic reaction mixtures catalyzes the formation of amide products, control reactions were performed on **4** and **5** in the absence of BSA. In both cases, only the corresponding amides were detected.

Kinetic parameters were measured spectrophotometrically for the alternative substrates shown in Table 1. The specificity constant k_{cat}/K_m for nitrosobenzene is of the same order of magnitude as that of the natural acceptor substrate, D-GAP. Reduced specificity constants were measured for the larger naphthol-containing substrates **5**–**8** (Table 1), an observation that is consistent with the idea that sterically demanding naphthol substrates could exhibit a reduction in efficiency of turnover as a consequence of reduced affinity for the enzyme. However,

Table 1. Substrate specificity of nitroso substrates.[a]

Substrate	k_{cat} [min^{-1}][b]	K_m [μM][b]	k_{cat}/K_m ($\times 10^4$) [$M^{-1} min^{-1}$]
D-GAP	102 ± 7	28 ± 4	364 ± 60
1	175 ± 19	133 ± 18	132 ± 20
3	36 ± 7	99 ± 16	36 ± 9
4	0.9 ± 0.1	54 ± 13	1.7 ± 0.5
5	1.1 ± 0.2	41 ± 10	2.7 ± 0.8
6	2.0 ± 0.2	24 ± 6	8 ± 2
7	1.18 ± 0.04	18 ± 4	6.6 ± 1.5
8	1.3 ± 0.2	63 ± 7	2.1 ± 0.4
9	1.4 ± 0.2	387 ± 18	0.36 ± 0.05

[a] Reaction conditions: 100 mM HEPES, pH 8.0, 2 mM $MgCl_2$, 5 mM NaCl, 1 mM ThDP, 1 mg mL^{-1} BSA, 10–20 mM pyruvate, 10% DMSO (*v*/*v*), 37 °C. [b] Performed in triplicate. Values shown are the average ± SEM.

detailed kinetic analysis of nitroso substrate turnover suggests this is not the case. Small nitrosobenzene analogues display higher reactivity (high k_{cat}) but lower affinity (higher K_m) relative to D-GAP (**1** and **3**, Table 1). Contrary to our expectations, several sterically demanding alternative substrates exhibit high affinities for DXP synthase, with nitrosonaphthols **5**–**8** showing comparable affinity to the natural substrate. In these cases, a reduced k_{cat} accounts for the lower turnover efficiency, in line with previous reports on the sensitivity of nitroso turnover to substituent effects.[26] The remarkably high affinities measured for sterically demanding substrates on DXP synthase is in stark contrast to previously reported trends in nitroso turnover by ThDP-dependent enzymes;[27] here increasing steric bulk of the substrate correlated with decreased affinity.

Aromatic nitroso substrates exhibit low affinity for the smaller PDH active site

As a basis for selective inhibitor design, we determined whether DXP synthase displays a higher affinity for sterically demanding substrates than PDH does. Thus, nitroso analogues **1**, **4** and **6** were evaluated as substrates for porcine PDH (Figures S10 and S11). Our results indicate these aromatic substrates exhibit significantly lower affinities for PDH than for DXP synthase (Table 2), in contrast to the trend observed for DXP synthase. Nitrosobenzene displays a 2.7-fold increase in K_m for PDH compared to DXP synthase, whereas the largest of the nitroso substrates tested, nitrosonaphthol **6**, displays an ap-

Table 2. Determination of K_m for nitroso substrates against *E. coli* DXP synthase (DXPS) compared to the porcine PDH E1 subunit.

Substrate	PDH K_m [μM][a]	K_m^{PDH}/K_m^{DXPS}
1	350 ± 30	2.7
4	408 ± 60	7.5
6	450 ± 16	19.3

[a] Reaction conditions: 100 mM HEPES, pH 8.0, 2 mM $MgCl_2$, 5 mM NaCl, 1 mM ThDP, 1 mg mL^{-1} BSA, 10–20 mM pyruvate, 10% DMSO (*v*/*v*), 37 °C. Performed in triplicate; values shown are the average ± SEM.

proximately 19-fold increase in K_m for PDH compared to DXP synthase. We hypothesized that the DXP synthase active site might be relatively larger to accommodate ternary complex formation during catalysis. Indeed, a comparison of active site volumes (calculated from crystal structure coordinates that were aligned in Coot[28] and then analyzed by using PocketFinder[29]) suggests the DXP synthase active site is significantly larger than those of the ThDP-dependent enzymes PDH or transketolase (Figures 2 and S12). The hydrophobic nature of the alternative nitroso substrates tested could potentially drive the selectivity of turnover by DXP synthase. However, when

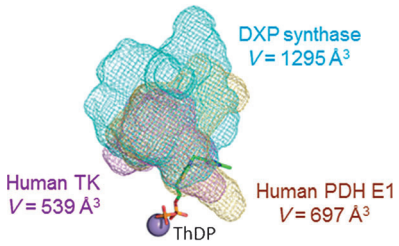

Figure 2. Overlay of the DXP synthase, transketolase (TK), and PDH E1 subunit active site pockets. The DXP synthase active site is predicted to be larger than the other two.

the active site pockets of DXP synthase, PDH, and TK were analyzed by using fpocket,[30] the computed hydrophobicity score (based on the hydrophobicity scale published by Monera et al.[31]) indicated that the PDH pocket is more hydrophobic than that of DXP synthase, whereas TK has the least hydrophobic pocket (Table S1). Taken together, these results suggest that the incorporation of sterically demanding fragments into inhibitor scaffolds could drive selective inhibition and is facilitated mostly by the larger cavity of DXP synthase.

Inhibition of DXP formation by nitroso alternative substrates

The low K_m values measured for aromatic nitroso substrates suggest that these analogues bind with reasonable affinity in the enzyme active site. Thus, we hypothesized that alternative substrates with aromatic scaffolds could also act as inhibitors of the natural reaction. Compounds **1** and **3**–**9** were evaluated as inhibitors of DXP synthase by using an HPLC-based assay previously reported.[18] Interestingly, all the nitroso compounds exhibited weak inhibitory activity with IC_{50} values ranging from 208 μM to >2 mM and with no apparent trend with measured K_m values (Table 3). As one of the higher-affinity substrates, the readily available nitrosonaphthol, **5**, was selected for further evaluation in an effort to understand the mechanism of inhibition. This inhibitor was found to exhibit a competitive inhibition pattern with respect to D-GAP (apparent $K_i = (422 \pm 80)$ μM, Figure S14). The more than tenfold difference between the K_m ((41 ± 10) μM) and K_i suggests that nitrosonaphthols could adopt a binding mode for turnover that is distinct from the binding mode for inhibition. Alternatively, K_i might reflect

Table 3. Inhibition of DXP formation by nitroso substrates.[a]

Substrate	IC_{50} [μM][b]	Substrate	IC_{50} [μM][b]
1	208 ± 20	**6**	522 ± 60
3	291 ± 11	**7**	354 ± 90
4	844 ± 170	**8**	>2000
5	1065 ± 190 (K_i=(422±80) μM)	**9**	>2000

[a] Reaction conditions: 100 mM HEPES, pH 8.0, 2 mM $MgCl_2$, 5 mM NaCl, 1 mM ThDP, 1 mg mL^{-1} BSA, 10% DMSO (*v*/*v*), 30 μM D-GAP, 80 μM pyruvate, 37 °C. [b] Performed in triplicate; values shown are the average ± SEM.

the affinity of the Michaelis–Menten complex between enzyme and nitrosonaphthol, whereas the K_m for this substrate could be indicative of a higher-affinity ternary complex further along the reaction coordinate in this two-substrate system.

Nitrosonaphthols and D-GAP adopt distinct binding modes during turnover

R478 and R420 are known to be essential for the binding of D-GAP, presumably by anchoring the phosphate group (unpublished results). Two DXP synthase variants (R478A and R420A) were evaluated as catalysts for C–N bond formation with nitrosonaphthols **5**–**7**. Although both of these mutations adversely affect the binding of D-GAP, they have no apparent effect on the affinities of nitroso substrates in C–N bond formation, as indicated by the comparable K_m values measured for both variant and wild-type enzymes with nitroso substrates (Table 4, Figure S15). This is consistent with the notion that nitrosonaphthols adopt a binding mode for turnover that is distinct from that of D-GAP.

Table 4. WT, R478A, and R420A catalyze comparable turnovers of nitrosonaphthols.[a]

Alternative substrate	K_m [μM] WT DXP synthase	R478A[b]	R420A[b]
5	41 ± 10	23 ± 4	32 ± 5
6	24 ± 6	20 ± 3	16 ± 1
7	18 ± 4	13 ± 1	14 ± 2

[a] Reaction conditions: 100 mM HEPES, pH 8.0, 2 mM $MgCl_2$, 5 mM NaCl, 1 mM ThDP, 1 mg mL^{-1} BSA, 10–20 mM pyruvate, 10% DMSO (*v*/*v*), 37 °C. [b] Performed in triplicate; values shown are the average ± SEM.

Selective inhibition of DXP synthase by benzyl acetylphosphonate (BnAP)

Our results suggest that the comparatively large active site of DXP synthase can accommodate sterically demanding scaffolds, but in a manner that does not interfere with DXP formation. On this basis, we hypothesized that aromatic components could be incorporated into unnatural bisubstrate analogues to

impart selectivity of inhibition against DXP synthase. To demonstrate this concept, we prepared benzyl acetylphosphonate (BnAP) as a potential selective inhibitor of DXP synthase. BnAP incorporates the acetyl phosphonate moiety as a pyruvate mimic and a benzyl group to mimic the alternative acceptor substrate, nitrosobenzene (Figure 3A). As expected, BnAP is a competitive inhibitor with respect to pyruvate with reasonable potency against DXP synthase ($K_i = (10.4 \pm 1.3)$ μM), and exhibits ~85-fold higher inhibitory activity against DXP synthase than PDH (Figure 3). Additionally, BnAP exhibits an uncompetitive inhibition pattern with respect to D-GAP ($K_i = (70 \pm 8)$ μM, Figure 3D). The requirement for D-GAP binding is consistent with the idea that aromatic scaffolds adopt a binding mode that is distinct from D-GAP.

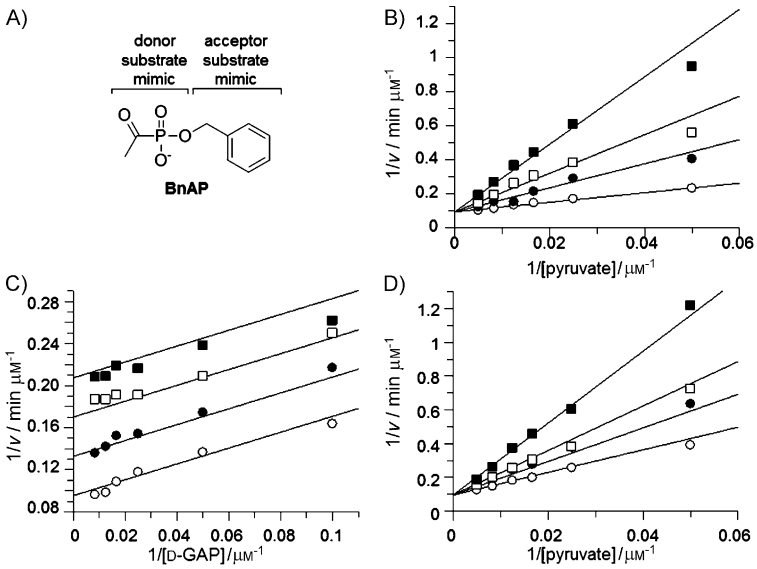

Figure 3. BnAP is a selective inhibitor of DXP synthase. A) Design of BnAP as a selective inhibitor of DXP synthase. B) BnAP is a competitive inhibitor of DXP synthase with respect to pyruvate ($K_i = (10.4 \pm 1.3)$ μM). The concentration of pyruvate was varied (20–200 μM) at several fixed concentrations of BnAP (0 (○), 15 (●), 30 (□) and 60 (■) μM) and 100 μM D-GAP; C) BnAP is an uncompetitive inhibitor of DXP synthase with respect to D-GAP ($K_i = (70 \pm 8)$ μM). The concentration of D-GAP was varied (10–120 μM) at fixed concentrations of BnAP (0 (○), 25 (●), 50 (□) and 75 (■) μM) and 200 μM pyruvate; D) BnAP is a competitive inhibitor of PDH with respect to pyruvate and exhibits selective inhibition against DXP synthase compared to PDH ($K_i^{PDH} = (882 \pm 78)$ μM, $K_i^{PDH}/K_i^{DXPS} \sim 85$). The concentration of pyruvate was varied (20–200 μM) at several fixed concentrations of BnAP (0 (○), 0.5 (●), 1 (□) and 2.25 (■) mM). Representative double reciprocal plots are shown.

Discussion

DXP synthase is an attractive drug target for the development of new anti-infective agents, and selective inhibitors of this enzyme are sought. Our study highlights C–N bond formation as a new reaction catalyzed by DXP synthase and shows nitroso substrates to be useful tools for probing the active site of this potential drug target. Our study shows that DXP synthase-catalyzed C–N bond formation can lead to the generation of hydroxamic acids and amides, with electron-rich nitroso substrates giving predominantly amide products. Although the mechanism for this transformation has not been elucidated, it is thought to occur through a hydroxamic acid intermediate.[25] Notably, we have demonstrated that nitroso substrate analogues with a naphthol scaffold exhibit an exceptional affinity for DXP synthase that is comparable to that of the natural acceptor substrate, D-GAP. Further, sterically demanding substrates are selectively turned over by DXP synthase and show a considerably lower affinity for the ThDP-dependent enzyme PDH. Consistent with this finding, calculations indicate that the volume of the DXP synthase active site is significantly greater than that of PDH or transketolase and can thus accommodate sterically demanding alternative substrates. The alternative acceptor substrates tested in this study are surprisingly weak inhibitors of DXP formation, with nitrosonaphthol (**5**) acting as a weak competitive inhibitor against D-GAP. The more than tenfold discrepancy between K_m and K_i for this compound suggests that multiple binding modes could be possible for **5**, or they could reflect a lower-affinity complex en route to a higher-affinity ternary complex (described by $K_m^{nitrosonaphthol}$). Evidence that nitrosonaphthols adopt a different binding mode from D-GAP during turnover was obtained through substitution of R478 and R420, active site residues that are essential for D-GAP binding. The variants R478A and R420A display efficient turnover and comparable affinity for nitrosonaphthols to wild-type DXP synthase. Further studies are needed to define the critical residues for C–N bond formation, and especially those that are important for aromatic substrate binding.

Taken together, the data suggest that incorporating an aromatic group into an unnatural bisubstrate analogue scaffold should give the analogue the ability to selectively inhibit DXP synthase over other ThDP-dependent enzymes. Indeed, benzylacetylphosphonate selectively inhibits DXP synthase with a K_i of (10.4 ± 1.3) μM and $K_i^{PDH}/K_i^{DXPS} \sim 85$. Although BnAP is comparable in inhibitory activity to butylacetylphosphonate,[18] an increase in K_i^{PDH}/K_i^{DXPS} is observed; this suggests sterically demanding aromatic acetylphosphonates as a promising new class of selective DXP synthase inhibitors.

Experimental Section

General: Unless otherwise noted, all reagents were obtained from commercial sources. HPLC analyses were performed on a Beckman Gold Nouveau System with a Grace Alltima 3 μm C18 analytical Rocket column (53 mm × 7 mm). Spectrophotometric analyses were carried out on a Beckman DU 800 UV/Vis spectrophotometer. Mass spectrometric analyses were either performed on Shimadzu LC-MS IT-TOF or Thermo Fisher Finnigan LCQ Classic spectrometer or obtained from the University of Illinois at Urbana–Champaign Mass Spectrometry Laboratory. All enzymatic reactions were carried out in low-retention microcentrifuge tubes to prevent the adsorption of hydrophobic substrates. All enzyme reaction mixtures contained 10% DMSO to solubilize hydrophobic substrates. These conditions have only a minimal impact on the natural reaction. Recombinant

DXP synthase was purified as previously described.[19] The protein concentration was determined by using the Bradford assay. Porcine pyruvate dehydrogenase was obtained from a commercial source; its specificity activity was determined by the manufacturer. For chemical synthesis, CH_2Cl_2 was distilled over calcium hydride. Anhydrous acetonitrile was packed in Sure-Seal bottles. All reactions were carried out under argon. NMR spectra were recorded on a Varian 500 MHz spectrometer. Reaction progress was monitored through ^{31}P NMR with triphenylphosphine oxide (TPPO, $\delta = 0$ ppm) dissolved in deuterated benzene as external standard. ^1H NMR chemical shifts are reported relative to tetramethylsilane (TMS, $\delta =$ 0 ppm) as internal reference. Preparative HPLC was performed on a Beckman Gold Noveau system with a Varian Dynamax 250× 21.4 mm Microsorb C18 column.

HPLC analysis of DXP synthase-catalyzed C–N bond formation and product characterization: Reaction mixtures containing HEPES (100 mM, pH 8.0, 2 mM $MgCl_2$, 5 mM NaCl), ThDP (1 mM), BSA (1 mg mL^{-1}), pyruvate (10–20 mM), DMSO (10%, *v/v*) and nitroso substrate (0.5–5 mM) were preincubated at 37 °C for 5 min. Reactions were initiated with enzyme (1–5 μM). Aliquots of the enzymatic mixture were removed at various time intervals and quenched in an equal volume of cold methanol. Quenched mixtures were incubated on ice for 20 min. Precipitated proteins were removed by centrifugation, and the supernatant was analyzed by HPLC with UV detection under the following conditions: flow rate = 3 mL min^{-1}, solvent A: NH_4OAc (100 mM, pH 4.6), solvent B: acetonitrile, method: 0–100% B over 10 min. The products were extracted from the supernatant with ethyl acetate (3×). The combined organic extracts were concentrated, and the resulting samples were dissolved in MeOH and resubjected to HPLC analysis to confirm that product degradation had not taken place during the extraction procedure. Products were subsequently characterized by mass spectrometry.

Determination of kinetic parameters for nitroso substrates: Reaction mixtures containing HEPES (100 mM, pH 8.0, 2 mM $MgCl_2$, 5 mM NaCl), ThDP (1 mM), BSA (1 mg mL^{-1}), pyruvate (10–20 mM), DMSO (10%, *v/v*), and nitroso substrate (10–300 μM) were preincubated at 37 °C for 5 min. Enzymatic reactions were initiated by addition of DXP synthase (0.5–2 μM; or 0.1 units per mL PDH) and monitored spectrophotometrically by measuring the rate of disappearance of the nitroso substrate at its corresponding λ_{max}. Substrate concentration as a function of time was determined from absorbance values by using Beer's Law. Initial reaction rates were determined from the linear range of the reaction progress curve, usually within 1–3 min. Data analysis to determine k_{cat} and K_m for each alternative substrate was carried out by using GraFit version 7 from Erithacus Software.

Evaluation of nitroso substrates as inhibitors of DXP formation: Reaction mixtures containing HEPES (100 mM, pH 8.0, 2 mM $MgCl_2$, 5 mM NaCl), ThDP (1 mM), BSA (1 mg mL^{-1}), DMSO (10%, *v/v*), D-GAP (30 μM), pyruvate (80 μM), and various concentrations of nitroso inhibitor were preincubated at 37 °C for 5 min. Enzyme reactions were initiated by addition of DXP synthase (0.1 μM). Aliquots (150 μL) of the enzymatic mixture were removed between 0.5 and 3 min and quenched in ice-cold methanol (150 μL). Precipitated protein was removed by centrifugation, and the supernatant was diluted in an equal volume of water. The nitroso substrate was removed by extraction into acetonitrile (3×) by using a previously described freeze-extraction technique.[32] The aqueous layer maintained a constant ratio of D-GAP and DXP during the extraction, and was subjected to derivatization conditions to produce the corresponding hydrazones with a fivefold excess of 2,4-dinitrophenylhydrazine[19] for 20 min to ensure complete derivatization of substrates and product at low concentration. The derivatization mixtures were analyzed by HPLC as previously described.[19] To determine the initial reaction rates in the presence of various inhibitor concentrations, the D,L-GAP and DXP hydrazone HPLC peak areas were measured, and the product concentration was determined as a percentage of total peak area and plotted against reaction time. Initial rates GraFit version 7 from Erithacus Software was used to generate IC_{50} curves.

Calculating the active site volume: Coordinates for the ThDP-dependent enzymes, *Deinococcus radiodurans* DXS (PDB ID: 2O1X),[16] human PDHE1p (PDB ID: 3EXE),[33] and transketolase (PDB ID: 3MOS)[34] were structurally aligned in Coot[28] by using LSQ Superpose and residue ranges A:151–164 (2O1X), E:164–177 (3EXE), and A:152–165 (3MOS). The choice of residues was based on their close proximity to ThDP in order to maximize a similar orientation of the active site region of interest. The RMS deviation, calculated with VMD[35] between residues lining the ThDP binding site, was 1.54 Å (2O1X/3EXE) or 1.01 Å (2O1X/3MOS) for 16 C_a backbone atoms. The biological assembly of transketolase (3MOS) was determined by using the PISA[36] web server. Aligned structures were uploaded to the Pocket-Finder[29] web server to determine the volumes of the active site pockets. Cofactors ThDP or ThDP + metal ions were treated as part of the protein, and all other molecules were discarded for the purpose of defining the protein surface for pocket detection. Pocket-Finder reported volumes and generated space-filling models for the active site pocket in each structure corresponding to the pocket adjacent to TDP in chain A of 2O1X. An overlay of the mesh representations with respect to the active site cofactor and metal ion was rendered in PyMOL (The PyMOL Molecular Graphics System, Version 1.5.0, Schrödinger, LLC).

Active site pocket hydrophobicity calculations with fpocket: Fpocket[30] (Table S1) was run to detect and analyze pockets in DXP synthase (2O1X), PDH (3EXE) and TK (3MOS). The complete coordinate files for DXP synthase and PDH, and the biological assembly for TK, were used as inputs for fpocket. The default cofactor list for fpocket was modified to include TDP and TPP prior to program compilation so that the ThDP cofactor would be treated as a part of the protein as opposed to a removable ligand. The pockets corresponding to the active sites used for the volume calculations with Pocket Finder were determined visually, and the parameters were recorded.

Synthesis of BnAP (Figure S16): Benzylacetylphosphonate was prepared starting from phosphorus trichloride in a similar manner to butylacetylphosphonate,[18] by using standard procedures. Tribenzyl phosphite was generated from benzyl alcohol, diisopropylethylamine, and phosphorous trichloride according to Saady et al.[37] The spectral properties of the compound were identical to published values. For the preparation of benzylacetylphosphonate (BnAP), a flame-dried flask, cooled under argon, was charged with acetyl chloride (0.32 mL, 4.5 mmol). Tribenzyl phosphite (0.46 g, 1.3 mmol) was dissolved in anhydrous CH_2Cl_2 (13 mL), and the resulting mixture was added dropwise to acetyl chloride. The progress of the reaction was monitored through ^{31}P NMR spectroscopy, and complete conversion of tribenzyl phosphite ($\delta = 113$ ppm) to dibenzylacetyl-phosphonate ($\delta = -26$ ppm) was observed within 1 h. Volatiles were removed in vacuo, and the crude material was used without further purification. Dibenzylacetylphosphonate was dissolved in anhydrous acetonitrile (2.2 mL), and lithium bromide (0.17 g, 0.95 mmol) was added in one portion. The reaction mixture was heated to 50 °C for ~4 h. The lithium salt of benzylacetylphosphonate precipitated from solution and was removed by

filtration. The filter cake was washed successively with cold acetonitrile and diethyl ether (20 mL portions of). The crude product was purified by reversed-phase preparative HPLC. Flow rate = 10 mL min^{-1}; solvent A: $HNEt_3OAc$ (50 mM, pH 6.0), solvent B: methanol, method 5–80% B over 75 min. The purity of fractions was determined by analytical RP-HPLC. Flow rate = 3 mL min^{-1}; solvent A: $HNEt_3OAc$ (50 mM, pH 6.0), solvent B: methanol, method 5–80% B over 12 min. Combined fractions were lyophilized to yield 0.0975 g BnAP as the triethylammonium salt (24% over two steps). ^{1}H NMR (D_2O): $\delta = 1.20$ (t, 9H), 2.31 (d, 3H), 3.11 (m, 6H), 4.91 (d, 2H), 7.35 ppm (m, 5H); ^{31}P NMR (D_2O): $\delta = -27.43$ ppm (s); HRMS (ESI): *m/z* calcd for $C_{15}H_{27}NO_4P$ (triethylammonium salt): 316.1678 $[M+H]^+$, found: 316.1673.

Inhibition of DXP synthase by BnAP: In order to evaluate the inhibitory activity of BnAP against DXP synthase, a continuous spectrophotometric coupled assay was used to measure formation of DXP by monitoring IspC consumption of NADPH (340 nm).[2] DXP synthase reaction mixtures (previously described) including BnAP (15, 30, and 60 μM), IspC (1 μM), and NADPH (100 μM) were preincubated at 37 °C for 5 min. Initial rates were measured after the reaction had been initiated by the addition of DXP synthase. Inhibition of the coupling enzyme (IspC) by BnAP was not observed at up to 1.5 mM. Experiments were performed in triplicate. Double reciprocal analysis of the data was carried out by using GraFit version 7 from Erithacus Software.

Inhibition of PDH by BnAP: Pyruvate dehydrogenase activity was measured spectrophotometrically as previously reported[38] by monitoring the absorbance changes at 340 nm caused by the reduction of NAD^+ by PDH. Reaction mixtures contained HEPES (100 mM, pH 8.0), BSA (1 mg mL^{-1}), ThDP (0.2 mM), coenzyme A (0.1 mM), $MgCl_2$ (1 mM), cysteine (2 mM), and tris(2-carboxyethyl)-phosphine (TCEP; 0.3 mM). The reaction was initiated with enzyme (0.01 units mL^{-1}), and activity was monitored at 30 °C. For inhibition studies, reaction mixtures (described above) including BnAP (0.5, 1, 2.25 mM) were preincubated at 30 °C for 5 min. Initial rates were measured immediately after reactions had been initiated by the addition of PDH (0.01 units mL^{-1}). Double reciprocal analysis of the data was carried out by using GraFit version 7 from Erithacus Software.

Acknowledgements

We gratefully acknowledge Katie Heflin for her efforts in the optimization of the HPLC assay used for the inhibition studies. Kip Bitok is acknowledged for synthesizing tribenzyl phosphite. This work was supported by funding from The Johns Hopkins Malaria Research Institute Pilot Grant (F.M.M. and C.F.M.), and the National Institutes of Health (GM084998 for C.F.M., F.M.M., R.J.V.; T32M08018901 for F.M.M., R.J.V., L.B., and AI094967 for F.M.M.) This work was partially funded through The Bloomberg Family Foundation (L.B. and J.B.).

Keywords: biosynthesis · DXP synthase · enzyme inhibitors · isoprenoids · kinetics · substrate specificity

[1] C. A. Testa, M. J. Brown, *Curr. Pharm. Biotechnol.* **2003**, *4*, 248–259.
[2] H. Jomaa, J. Wiesner, S. Sanderbrand, B. Altincicek, C. Weidemeyer, M. Hintz, I. Turbachova, M. Eberl, J. Zeidler, H. K. Lichtenthaler, D. Soldati, E. Beck, *Science* **1999**, *285*, 1573–1576.
[3] M. Rohmer, M. Knani, P. Simonin, B. Sutter, H. Sahm, *Biochem. J.* **1993**, *295*, 517–524.
[4] G. A. Sprenger, U. Schörken, T. Wiegert, S. Grolle, A. A. de Graaf, S. V. Taylor, T. P. Begley, S. Bringer-Meyer, H. Sahm, *Proc. Natl. Acad. Sci. USA* **1997**, *94*, 12857–12862.
[5] T. Kuzuyama, M. Takagi, S. Takahashi, H. Seto, *J. Bacteriol.* **2000**, *182*, 891–897.
[6] J. M. Estevez, A. Cantero, A. Reindl, S. Reichler, P. Leon, *J. Biol. Chem.* **2001**, *276*, 22901–22909.
[7] M. Harker, P. M. Bramley, *FEBS Lett.* **1999**, *448*, 115–119.
[8] A. C. Brown, M. Eberl, D. C. Crick, H. Jomaa, T. Parish, *J. Bacteriol.* **2010**, *192*, 2424–2433.
[9] L. M. Lois, N. Campos, S. R. Putra, K. Danielsen, M. Rohmer, A. Boronat, *Proc. Natl. Acad. Sci. USA* **1998**, *95*, 2105–2110.
[10] R. E. Hill, K. Himmeldirk, I. A. Kennedy, R. M. Pauloski, B. G. Sayer, E. Wolf, I. D. Spenser, *J. Biol. Chem.* **1996**, *271*, 30426–30435.
[11] L. M. Eubanks, C. D. Poulter, *Biochemistry* **2003**, *42*, 1140–1149.
[12] H. Patel, N. S. Nemeria, L. A. Brammer, C. L. Freel Meyers, F. Jordan, *J. Am. Chem. Soc.* **2012**, *134*, 18374–18379.
[13] L. A. Brammer, J. M. Smith, H. Wade, C. F. Meyers, *J. Biol. Chem.* **2011**, *286*, 36522–36531.
[14] R. A. Frank, F. J. Leeper, B. F. Luisi, *Cell. Mol. Life Sci.* **2007**, *64*, 892–905.
[15] R. Kluger, K. Tittmann, *Chem. Rev.* **2008**, *108*, 1797–1833.
[16] S. Xiang, G. Usunow, G. Lange, M. Busch, L. Tong, *J. Biol. Chem.* **2007**, *282*, 2676–2682.
[17] J. Mao, H. Eoh, R. He, Y. Wang, B. Wan, S. G. Franzblau, D. C. Crick, A. P. Kozikowski, *Bioorg. Med. Chem. Lett.* **2008**, *18*, 5320–5323.
[18] J. M. Smith, R. J. Vierling, C. F. Meyers, *MedChemComm* **2012**, *3*, 65–67.
[19] L. A. Brammer, C. F. Meyers, *Org. Lett.* **2009**, *11*, 4748–4751.
[20] M. Pohl, B. Lingen, M. Müller, *Chem. Eur. J.* **2002**, *8*, 5288–5295.
[21] M. Müller, D. Gocke, M. Pohl, *FEBS J.* **2009**, *276*, 2894–2904.
[22] A. S. Demir, P. Ayhan, S. B. Sopaci, *Clean Soil Air Water* **2007**, *35*, 406–412.
[23] M. D. Corbett, J. E. Cahoy, B. R. Chipko, *J. Natl. Cancer Inst.* **1975**, *55*, 1247–1248.
[24] M. D. Corbett, B. R. Chipko, *Bioorg. Chem.* **1980**, *9*, 273–287.
[25] M. D. Corbett, B. R. Corbett, *Bioorg. Chem.* **1982**, *11*, 328–337.
[26] M. D. Corbett, B. R. Corbett, *Biochem. Pharmacol.* **1986**, *35*, 3613–3621.
[27] a) T. Yoshioka, T. Uematsu, *Biochem. J.* **1993**, *290*, 783–790; b) P. Ayhan, A. S. Demir, *Adv. Synth. Catal.* **2011**, *353*, 624–629.
[28] P. Emsley, K. Cowtan, *Acta Crystallogr. Sect. D Biol. Crystallogr.* **2004**, *60*, 2126–2132.
[29] M. Hendlich, F. Rippmann, G. Barnickel, *J. Mol. Graphics Modell.* **1997**, *15*, 359–363.
[30] V. Le Guilloux, P. Schmidtke, P. Tuffery, *BMC Bioinf.* **2009**, *10*, 168.
[31] O. D. Monera, T. J. Sereda, N. E. Zhou, C. M. Kay, R. S. Hodges, *J. Pept. Sci.* **1995**, *1*, 319–329.
[32] M. Yoshida, A. Akane, *Anal. Chem.* **1999**, *71*, 1918–1921.
[33] M. Kato, R. M. Wynn, J. L. Chuang, S. C. Tso, M. Machius, J. Li, D. T. Chuang, *Structure* **2008**, *16*, 1849–1859.
[34] L. Mitschke, C. Parthier, K. Schröder-Tittmann, J. Coy, S. Ludtke, K. Tittmann, *J. Biol. Chem.* **2010**, *285*, 31559–31570.
[35] W. Humphrey, A. Dalke, K. Schulten, *J. Mol. Graphics* **1996**, *14*, 33–38.
[36] E. Krissinel, K. Henrick, *J. Mol. Biol.* **2007**, *372*, 774.
[37] M. Saady, L. Lebeau, C. Mioskowski, *Helv. Chim. Acta* **1995**, *78*, 670–678.
[38] S. Strumilo, J. Czerniecki, P. Dobrzyn, *Biochem. Biophys. Res. Commun.* **1999**, *256*, 341–345.

Received: March 27, 2013
Published online on July 3, 2013